Atmos. Chem. Phys., 4, 169–182, 2004
www.atmos-chem-phys.org/acp/4/169/
SRef-ID: 1680-7324/acp/2004-4-169

Atmospheric Chemistry and Physics

Role of the NO_3 radicals in oxidation processes in the eastern Mediterranean troposphere during the MINOS campaign

M. Vrekoussis[1], M. Kanakidou[1], N. Mihalopoulos[1], P. J. Crutzen[2], J. Lelieveld[2], D. Perner[2], H. Berresheim[3], and E. Baboukas[2]

[1]Environmental Chemical Processes Laboratory, Department of Chemistry, University of Crete, P.O. Box 1470, 71409 Heraklion, Greece
[2]Max-Planck-Institute for Chemistry, Air Chemistry Department, P.O. Box 3060, 55020 Mainz, Germany
[3]German Weather Service, Meteorological Observatory, Hohenpeissenberg, Albin-Schwaiger-Weg 10, Germany

Received: 26 March 2003 – Published in Atmos. Chem. Phys. Discuss.: 19 June 2003
Revised: 27 September 2003 – Accepted: 21 January 2004 – Published: 3 February 2004

Abstract. During the MINOS campaign (28 July–18 August 2001) the nitrate (NO_3) radical was measured at Finokalia station, on the north coast of Crete in South-East Europe using a long path (10.4 km) Differential Optical Absorption Spectroscopy instrument (DOAS). Hydroxyl (OH) radical was also measured by a Chemical Ionization Mass-Spectrometer (Berresheim et al., 2003). These datasets represent the first simultaneous measurements of OH and NO_3 radicals in the area. NO_3 radical concentrations ranged from less than 3×10^7 up to 9×10^8 radicals$\cdot$ cm^{-3} with an average nighttime value of 1.1×10^8 radicals$\cdot$ cm^{-3}.

The observed NO_3 mixing ratios are analyzed on the basis of the corresponding meteorological data and the volatile organic compound (VOC) observations which were measured simultaneously at Finokalia station. The importance of the NO_3 radical chemistry relatively to that of OH in the dimethylsulfide (DMS) and nitrate cycles is also investigated. The observed NO_3 levels regulate the nighttime variation of DMS. The loss of DMS by NO_3 during night is about 75% of that by OH radical during day. NO_3 and nitrogen pentoxide (N_2O_5) reactions account for about 21% of the total nitrate ($HNO_{3(g)}$+$NO^-_{3(g)}$) production.

1 Introduction

The quality of the air and climate depend on the emissions, chemical transformation and deposition of trace constituents in the atmosphere. The self-cleaning efficiency of the troposphere is important to conserve air quality both during day and night. The most important oxidant species that regulate the self-cleaning efficiency of the troposphere are the OH radical, the NO_3 radical and ozone.

During the day, OH plays a decisive role in the cleaning mechanism of the atmosphere. During the night its concentration is, in most situations, negligible, thus, NO_3 radicals and O_3 are the main oxidants (e.g. Platt et al., 1984; Wayne et al., 1991; Poisson et al., 2001). NO_3 reacts with a number of VOCs initiating their night time degradation (Atkinson et al., 2000). It also contributes to the removal of NO_x (Allan et al., 1999) mainly via nitric acid (HNO_3) and particulate nitrate formation.

Regardless their importance, measurements of OH and NO_3 are scarce as they have been proven difficult due to the very low concentrations and the high spatial and temporal variability of these radicals. However, the DOAS measurements average over a few minutes of time and a few kilometres of distance (see Sect. 2.1) and thus partially integrate the time and space variability of the radical. The relative contribution of these two radicals to the oxidation efficiency of the atmosphere requires further investigation.

The major source of NO_3 is the oxidation of nitrogen dioxide (NO_2) by ozone (O_3):

$$NO_2 + O_3 \longrightarrow NO_3 + O_2 \quad (1)$$

The production rate of NO_3 (P_{NO_3}) by this reaction is given by $P_{NO_3}=k_{NO_2+O_3}\cdot[NO_2]\cdot[O_3]$ and equals 0.072 ppbv NO_3 per hour, for 0.5 ppbv of NO_2 and 50 ppbv of O_3 at 298 K, conditions typical of the Mediterranean area during summertime.

During the day, NO_3 has a very short lifetime (about 5 s) due to its strong absorption in the visible region of the solar spectrum (maximum absorption at 662 nm) and its rapid

Correspondence to: M. Kanakidou
(mariak@chemistry.uoc.gr)

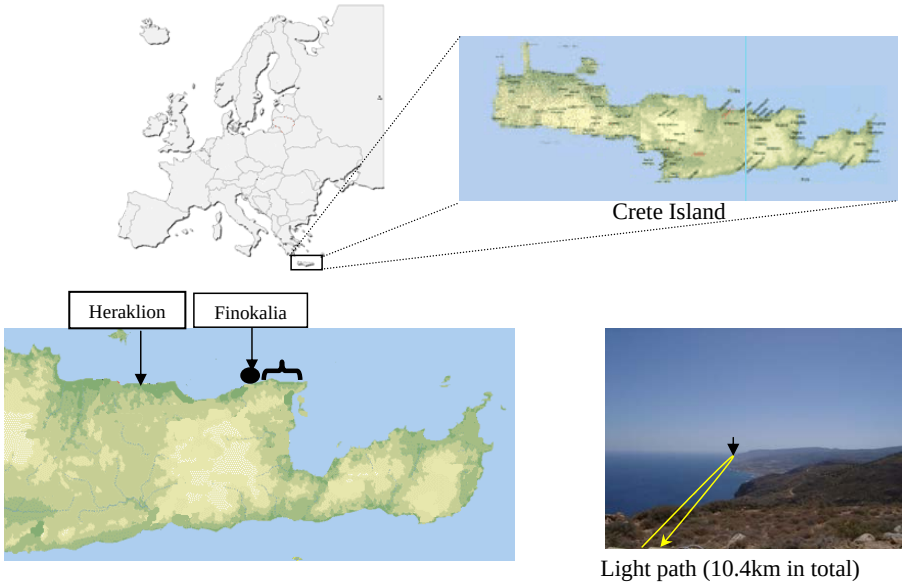

Fig. 1. Location of the Finokalia station, the retroreflectors and an indication of the light path of the DOAS instrument during the experiment.

photodissociation, mainly to NO_2 (Reaction 2a) and to a lesser extent to NO (Reaction 2b):

$$NO_3 + h\nu \longrightarrow NO_2 + O(^3P) \quad (2a)$$

$$NO_3 + h\nu \longrightarrow NO + O_2 \quad (2b)$$

In mid-latitudes near the surface the combined photolysis rate of the Reactions (2a) and (2b) is about J_2=0.2 s^{-1}=720 h^{-1} at noon during summer. Assuming dynamic equilibrium of NO_3 (production by Reaction (1) equals loss by photo-dissociation (2a and 2b)), the daytime concentration of NO_3 is calculated to be 0.1 pptv (PNO_3/J_2=[72 pptv h^{-1}]/[720 h^{-1}]). Such low NO_3 levels cannot be detected by the DOAS instrument as will be discussed later.

In the presence of NO, NO_3 is rapidly converted to NO_2 via Reaction (3). At 298 K and for a NO concentration of about 0.3 ppbv, the Reaction (3) is equivalent to the NO_3 loss via photo dissociation J_2 in mid latitudes at noon:

$$NO + NO_3 \longrightarrow 2NO_2 \quad (3)$$

NO_3 reacts with NO_2 to produce N_2O_5 via the temperature-dependent equilibrium (Waengberg et al., 1997):

$$NO_3 + NO_2 + M \rightleftharpoons N_2O_5 + M \quad (4)$$

Subsequent removal of nitrogen pentoxide (N_2O_5) leads to a net loss of NO_3 from the atmosphere. In the gas phase N_2O_5 can contribute to nitric acid formation following first and second order reactions with water vapour (Wahner et al., 1998; Atkinson et al., 2003; http://www.iupac-kinetic.ch.cam.ac.uk/):

$$N_2O_5 + H_2O \rightarrow 2HNO_3 \quad (5a)$$

$$N_2O_5 + 2H_2O \longrightarrow 2HNO_3 + H_2O \quad (5b)$$

The rates of the above reactions remain rather uncertain since the temperature dependence of these rates is not satisfactorily documented (Dimitroulopoulou and Marsh, 1997). Thus, the Wahner et al. (1998) temperature independent estimates, which are recommended by Atkinson et al. (2002), are used in the present study. Note also that Sander et al. (2003; JPL recommendations) give a slightly higher upper limit of 2×10^{-21} for the first order Reaction (5a). They also point out the large difficulty in distinguishing between the gas phase and the heterogeneous reactions of N_2O_5 with water and mention that the rate of (5a) could be 4 times lower, as has been measured by Sverdrup et al. (1987). This fourfold uncertainty is taken into account in the following discussion.

Additional HNO_3 formation paths involve VOC reactions with NO_3 and particularly DMS, aldehydes and higher alkanes (through the H abstraction mechanism) as well as heterogeneous reactions of NO_3 or N_2O_5 on particles (Heintz et al., 1996). The NO_3 reaction with unsaturated VOC proceeds via addition of NO_3 to the double C bond and does not produce HNO_3.

Several authors reported important interactions between nitrogen and sulfur cycles in the marine atmosphere via the NO_3 radical (Yvon et al., 1996; Carslaw et al., 1997; Allan et al., 1999; 2000). For instance, Allan et al. (1999) calculated that at NO_x levels exceeding 100 pptv, conditions typical of the marine atmosphere in the Northern Hemisphere, OH and NO_3 radicals are expected to equally contribute to the loss of DMS. The NO_3 radical contributes also to HNO_3 production during night as was shown by several studies including Heintz et al. (1996), Mentel et al. (1996), Allan et al. (2000), Geyer and Platt (2002).

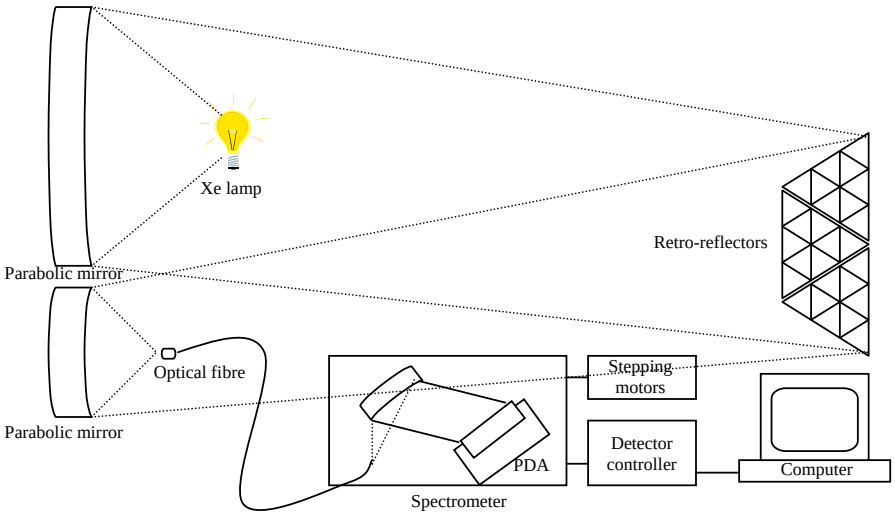

Fig. 2. Sketch of the long path DOAS system.

As part of the MINOS experiment daily measurements of ambient NO_3 concentrations were conducted during summer 2001, at the ground level station at Finokalia on the north-eastern coast of Crete. The aim was to study the NO_3 occurrence in the Mediterranean marine boundary layer, to evaluate the NO_3 role in the oxidation efficiency of the atmosphere and provide insights in the interactions between S and N cycles. To achieve these goals simultaneous measurements of OH, DMS, NO_2, gaseous HNO_3 and particulate NO_3 have been performed during a one month period.

2 Experimental

2.1 Setup of the long path DOAS instrument

The NO_3 radical mixing ratio has been monitored continuously by using a long path DOAS instrument at Finokalia (35.3′ N, 25.3′ E), Crete, Greece, 150 m above sea level, from 28 July to 18 August 2001 (Fig. 1). The monitoring station of the University of Crete at Finokalia is located 70 km eastward of Heraklion (137 000 inhabitants) and 25 km west of Agios Nikolaos (19 000 inhabitants), the nearest big towns in the area. These towns do not have any noticeable influence on the site due to the prevailing north winds.

The DOAS instrument used during MINOS was provided by the Max-Plank-Institute for Chemistry in Mainz and has been used in the past in several campaigns. The details of its operation have been presented elsewhere (Martinez et al., 2000); here only a short description is given. The DOAS uses a parabolic mirror behind a Xenon high pressure lamp (supplied by Hanovia, 500 W) to produce a parallel light beam (Fig. 2). At a distance of 5.2 km, an array of 30 retro-reflectors of 5 cm diameter reflects the main beam backwards to the sending point (total light path is 10.4 km) where another parabolic mirror focuses the light to the optical fibre in front of the collecting mirror. The reflectors are located near the sea surface (about 10 m asl) so the DOAS measurements correspond to average concentrations within the first 150 m a.s.l. Through an optical fibre (inner diameter 600 μm) the light is transmitted to the spectrograph and then to the detector. The spectrograph is based on a holographic lattice of the Fa. American Holographic (455.01, 240–800 nm) with a focal length of 212 mm, a linear dispersion of 7 nm mm^{-1} and a diffraction grating with 550 grooves mm^{-1}. The detector used to record the data is a 1024 pixel photodiode array (PDA, RY-1024, Hamamatsu), fixed to the focal plane of the spectrograph and cooled to -20°C to minimize the dark current.

The spectrum (N) used for the calculation of the species of interest has been obtained using the following equation:

$$\mathrm{N}=\frac{M-S}{L-O}$$

where:

- M is the atmospheric spectrum measured when the light path is focused on the centre of the fibre and contains scattered light,
- S is a spectrum of the atmospheric background due to scattered light measured by mechanically shifting the focus of the collecting mirror about 1 cm away from the optical fibre,
- O is the offset measured when the fibre is lidded by a black cover,
- L is the Lamp spectrum measured when the fibre is mounted directly to the lamp.

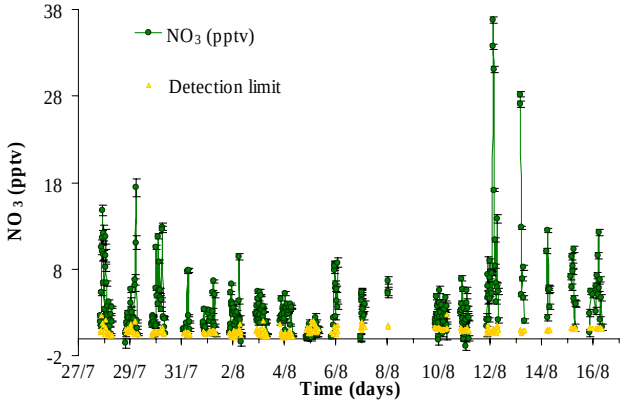

Fig. 3. NO_3 time series (in pptv) obtained at Finokalia during the MINOS campaign.

Note that after each S spectrum measurement the light is refocused on the focal point using an optimisation procedure that is computer controlled. Since a S spectrum is taken before each individual measurement, several S spectra are used for an integrated 30-min averaged measurement.

The N spectrum is then smoothed by fast Fourier transform, firstly with a high pass frequency filter and secondly, with a low pass frequency filter in order to remove i) high-frequency noise from the variability of the diode arrays, ii) adjacent broader spectral trends caused by Rayleigh and Mie scattering in the atmosphere and iii) detector etaloning. Every measurement is the mean value of nineteen individual ones and, on average, lasted 30 minutes.

The method used to obtain the final spectrum containing the information for the species of interest is the multi-scanning technique described in detail by Martinez-Harder (1998) and Brauers et al. (1995).

The NO_3 radical is detected in the visible spectral range. Two absorption peaks have been identified in the red region at 662 and 623 nm. In this work both NO_3 absorption bands are used for the NO_3 evaluation procedure and the band ($B_2E'-X^2A_2'$) at 662 nm is used for the quantification. Apart from the NO_3 radical, the main absorbers in that region (620–670) nm are water vapour and NO_2, and these species are fitted along with NO_3 in the analysis routine. The influence of water is much more critical for NO_3 than that of NO_2 because overtone vibrational bands of water peak at 651.5 nm, very close to NO_3. Since the concentration of NO_3 during daytime is negligible due to its rapid photolysis, daytime reference spectra (collected several times per day) are used as references for the humidity in the deconvolution procedure. These reference spectra for H_2O and NO_2 were then fitted simultaneously with the NO_3 reference spectrum to derive the NO_3 radical signature using a least-squares fitting routine that employs singular value decomposition. The thus derived optical density of this peak and the NO_3 cross sections reported by Yokelson et al. (1994) are used to determine NO_3 radical concentration. The instrumental noise (σ) that determines the detection limit of the method leads to a detection limit (3σ) of 1.2 pptv. Note that the few negative NO_3 values that have been calculated with this procedure have absolute values that are always below the detection limit of the method. These values are depicted in Fig. 3 that presents NO_3 observations by the DOAS instrument integrated approximately every 30 min during the whole campaign. The negative values are not taken into account for the interpretation and discussion of the results. Missing data were due to power breakdown or to drift of the focal point of the instrument during operation.

Nitrogen dioxide was measured also using the DOAS technique. The procedure is similar as the one described above for the NO_3 except that NO_2 has also clear peaks in the UV region. NO_2 was calculated from its peak at 405 nm with a cross section of 6.38×10^{-19} cm^2 (Yoshino et al, 1997). The mean instrumental noise (σ) in the case of NO_2 has been estimated to be 80 pptv, which leads to a detection limit (3σ) of 240 pptv.

2.2 Ancillary measurements

DMS was collected into 6-liter stainless steel electropolished canisters and analysed following the procedure described in details by Kouvarakis and Mihalopoulos (2000) and Bardouki et al. (2004). One sample was sampled and analysed per hour and the detection limit was 1 pptv.

Gaseous HNO_3 was analysed using the nebulization/reflux (Cofer mist) technique described in Cofer et al. (1985) and Sciare and Mihalopoulos (1999). A 0.5 μm PTFE filter was mounted in front of the Cofer line to collect aerosols. Gaseous HNO_3 was trapped by the mist and was analyzed as nitrate by Ion Chromatography. Simultaneously the PTFE filter situated in front of the Cofer sampler was extracted with MQ-water and analysed for nitrate using Ion Chromatography. Details on the analytical procedure can be found in Kouvarakis et al. (2000).

The meteorological data was obtained by an automatic meteorological station, which recorded ambient air temperature (T), relative humidity (RH), wind speed, wind direction and the direct solar radiation. The available data during the MINOS related to the NO_3 analysis and the corresponding analytical techniques, instruments and detection limits are summarised in Table 1.

3 Results

3.1 Measurements

The measured temporal profile of the NO_3 radical levels from 28 July to 17 August 2001 is shown in Fig. 3 together with the calculated detection limit (3 times the noise). A large daily as well as hourly variability of NO_3 has been observed,

Table 1. Measurements during MINOS relevant to the present analysis.

Measurement	Technique	Detection limit – Time resolution needed
NO, NO_y	Chemiluminescent detector	50 pptv–5 min
NO_2	DOAS	250 pptv–15 min
NO_3	DOAS	1.5 pptv–30 min
HNO_3	Nebulisation/reflux – IC	20 pptv–3 h
O_3	UV photometer	1 ppbv–5 min
DMS	GC-FPD	1 pptv–60 min
OH	Chemical Ionization Mass Spectrometry (SI/CIMS)	2.4×10^5 rad/cm^3 (2σ)-5 min
T, R.H., wind speed, wind direction, solar irradiance	Meteorological station	5 min
$J(NO_2)$, $J(O^1D)$	$2pi$ radiometer	5 min

Table 2. Observations of NO_3 radicals in the boundary layer.

Site	Coordinates	NO_3 Average (pptv)	NO_3 Maximum (pptv)	Total path (km)	Year (summer)	Ref.
Continental Boundary Layer						
Lindenberg	52°13′N–14°07′ E	4.6	85	10	1998	Geyer et al., 2001
Marine Boundary Layer						
Tenerife	28°40′ N–16°05′ W	8	20	9.6	1994	Carslaw et al., 1997
Kap Arkona (Rügen Island)	54°30′ N–13°30′ E	6–10	98	7.3	1993/94	Heintz et al., 1996
Wayborne Clean conditions	52°57′ N–1°08′ E	6	–	5	1995	Allan et al., 1999
Mace Head	53°19′ N, 9°54′ W	5	40	8.4	1996	Allan et al., 2000
Finokalia	35°30′ N, 25°7′ E	4.5	37	10.4	2001	This work

ranging from values below the detection limit (1.2 pptv) up to 37 pptv. The highest values have been observed during the night of 11 to 12 August 2001. This event will be discussed below. Table 2 presents NO_3 radical measurements reported for various locations around the world and compares them with the data obtained during this study. In general, the NO_3 observations at Finokalia station appear to be within the range of the reported data for the marine boundary layer.

3.2 Diurnal variation of NO_3

Daytime NO_3 levels were below the detection limit throughout the campaign (Fig. 4). NO_3 increases during sunset and reaches up to several tens of pptv during night. It decreases rapidly again during sunrise due to photodissociation. Similar diurnal tendencies have been reported by several authors in coastal areas (Heintz et al., 1998; Allan et al., 1999, 2000).

For comparison, Fig. 4 presents the mean diurnal variation of OH radicals (blue line) during the campaign. A detailed presentation of the OH measurements can be found in Berresheim et al. (2003). OH levels showed a strong diurnal variability with maxima

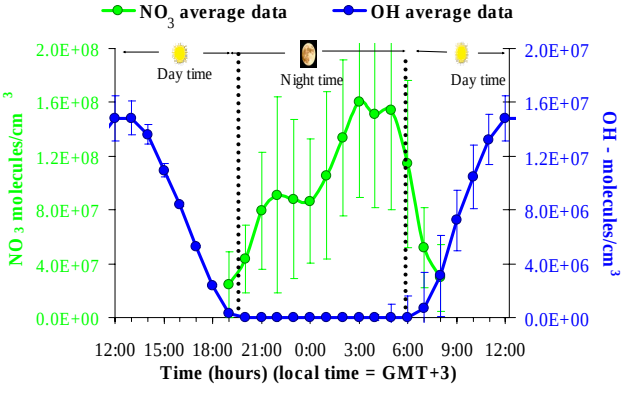

Fig. 4. Mean diurnal profile of the NO_3 radical concentration during the MINOS campaign. For comparison, OH radicals simultaneous measured are also reported. Note the factor of 10 between the two scales.

(approximately 2×10^7 molecules cm^{-3}) occurring around 12:30 local time and nighttime values below the detection limit. During the entire OH measurement period

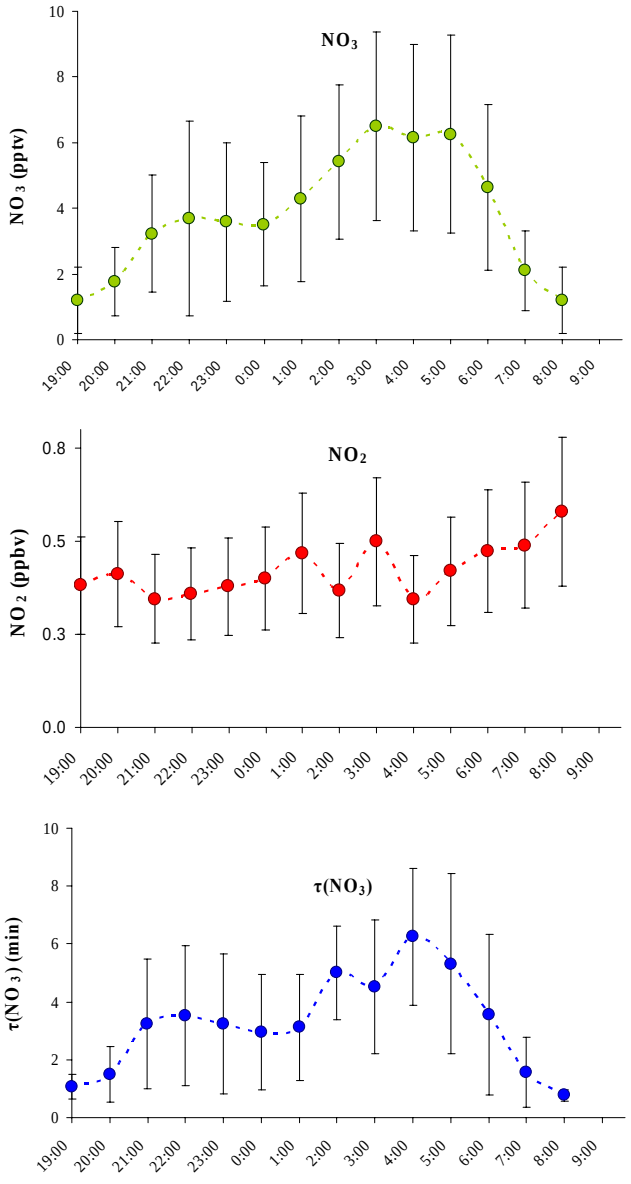

Fig. 5. Hourly mean observations and standard deviation **(a)** of NO_3in pptv, **(b)** of NO_2 in ppbv and **(c)** lifetime of NO_3 radicals in min – see text – during the MINOS campaign.

(6–21 August), the daytime mean and standard deviation were 8.2 $(\pm 1.6)\times 10^6$ molecules cm^{-3}, i.e. a factor of 13 lower than the nighttime NO_3 levels (1.1 $(\pm 1.1)\times 10^8$ molecules cm^{-3}). Most of the reactions of NO_3 with VOCs have rate constants that are between 5 and 1000 times slower than the corresponding reactions with OH (Atkinson et al., 2003, IUPAC recommendations). Thus according to the NO_3 and OH levels observed during this study the destruction rates of some VOCs are more important during the night than during daytime.

A very useful diagnostic tool for analyzing field observations of NO_3 is to calculate the atmospheric lifetime of the radical. As suggested by Platt et al. (1980), when NO_3 chemistry is in steady state, its lifetime $\tau(NO_3)$ is given by:

$$\tau(NO_3)=[NO_3]_{ss}/(K_{NO_2+O_3}[NO_2][O_3]) \quad (6)$$

The mean values (with one standard deviation) of NO_3 and NO_2 observed during the campaign and used to calculate the lifetime $\tau(NO_3)$ are depicted in Figs. 5a and b. The calculated $\tau(NO_3)$ during the MINOS campaign is found to range between 1 and 6 min; Fig. 5c. This very short lifetime of NO_3 actually supports the steady state assumption and is reproduced by the modelling study presented in Sect. 3.5. The steady state assumption does not exclude that NO_3 or N_2O_5 are transported to/from the sampling site from/to areas with different air temperatures. Under the experimental conditions NO_3 and N_2O_5 interconvert very fast to reach equilibrium with levels that depend on temperature and the NO_2 concentrations. For the high temperatures occurring during the MINOS experiment and for the geometric mean NO_2 levels observed during the MINOS campaign, the turnover times of NO_3 and N_2O_5 for the Reactions (4) range from 1–1.5 min and from 6–27 s respectively (Table 3). With such short turnover times, equilibrium is reached in less than 2 min.

The calculated $\tau(NO_3)$ is in good agreement with the average of 4.2 min reported by Heintz et al. (1996) from long-term observations of NO_3 at the island of Rügen in the Baltic Sea. The balance between the production and loss of NO_3 can also be investigated by correlating NO_3 levels with the production rate $P(NO_3)$. No significant correlation was observed during the MINOS campaign indicating that the N_2O_5 sink is regulating the NO_3 levels (Martinez et al., 2000; Heintz et al., 1996). In addition, a good negative correlation has been observed between the calculated $\tau(NO_3)$ and the NO_2 ($\tau(NO_3)=-0.94\,[NO_2]+4.42$, $r^2=0.82$) as in Heintz et al. (1996) indicating that NO_3 is mainly removed via transformation to N_2O_5 and subsequent loss of N_2O_5 by reactions with water vapour and heterogeneous reactions. This conclusion is also supported by the model simulations presented in

Table 3. Rates constants for the reactions (4, k_4) and (-4, k_{-4}), their ratio k_4/k_{-4} at the minimum and maximum temperatures observed during MINOS and the corresponding NO_2 levels at which the NO_3 and the N_2O_5 levels are equal. The reported lifetimes have been calculated on the basis of the geometric mean observed NO_2 mixing ratio of 0.4 ppbv.

	T min (22.5°C)	T max (30.2°C)
k_4 (molecules^{-1} cm^3 s^{-1}) $NO_2+NO_3\rightarrow N_2O_5$	1.39×10^{-12}	2.02×10^{-12}
k_{-4} (s^{-1}) $N_2O_5\rightarrow NO_2+NO_3$	3.67×10^{-2}	1.66×10^{-1}
k_4/k_{-4}	2.63×10^{10}	8.21×10^{10}
NO_2 (ppbv) for NO_3/N_2O_5=1	1.07	3.35
$\tau_{N_2O_5\_k-4}$ (s)	27	6
$\tau_{NO_3\_k4}$(s)	92	63

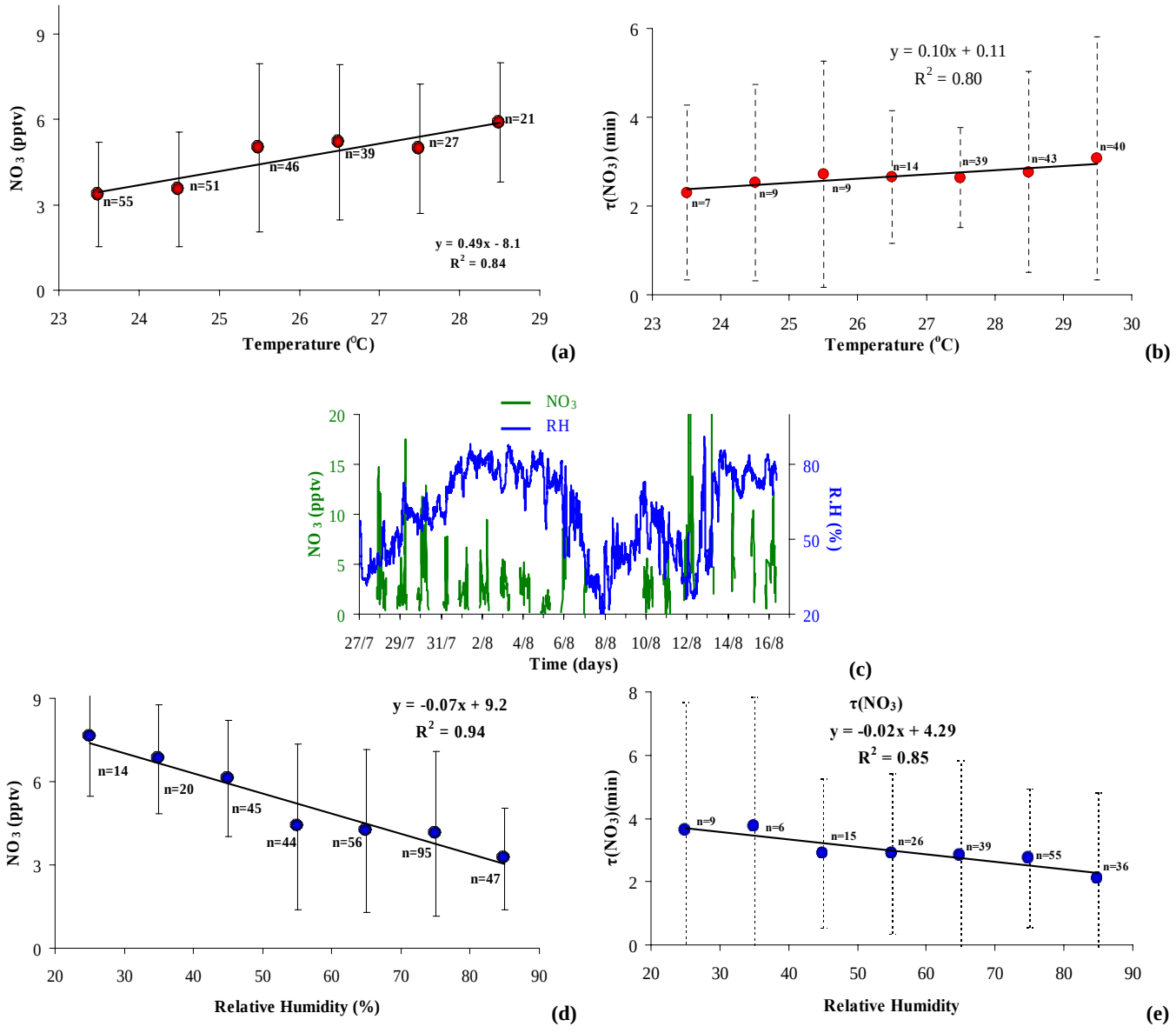

Fig. 6. **(a)** correlation between NO_3 (in pptv) and air temperature (°C) with NO_3 values integrated every 10 units of temperature; **(b)** correlation between NO_3 lifetime and air temperature (°C) with values integrated every 10 units of temperature **(c)** Time series of NO_3 and Relative Humidity (RH in %) during the campaign, **(d)** correlation between NO_3 and RH with NO_3 values integrated every 10 units of RH and **(e)** correlation between NO_3 lifetime and RH.

Sect. 3.5 and by the effect of temperature and relative humidity (RH) on NO_3 levels that are discussed in detail in the following paragraphs.

3.3 Meteorological parameters and their impact on NO_3

Temperature, relative humidity (RH), wind direction and speed and solar radiation were continuously monitored at Finokalia during the MINOS campaign. Temperature ranged between 22.5°C and 31.5°C (mean=25.7°C), whereas RH varied from 20 to 90% (mean=62%). The temperature changes observed during MINOS (9°C between the maximum and minimum temperature) are expected to affect NO_3 variability. Indeed, the rates of the NO_3 conversion to N_2O_5 (Reaction 4) and of the thermal decomposition of N_2O_5 (Reaction 4) as well as the equilibrium rate (k_4/k_{-4}) strongly depend on temperature as shown in Table 3. On the other hand, for the range of temperatures in Table 3 the production rate of NO_3 from the O_3 reaction with NO_2 presents 2.5–3.5 times smaller temperature dependence (the rate of Reaction (1) is

Table 4. Gas phase reactions involved in the NO_3 radical budget. T is air temperature in Kelvin, AIR is air density in molecules cm^{-3} and $[O_2]$ is O_2 concentration in molecules cm^{-3}. The reaction rate of the OH-initiated DMS oxidation is also given for comparison purposes.

Reaction	Rate	Rate at 298 K
	NO_3 production	
$NO_2+O_3 \rightarrow NO_3+O_2$	$1.4\times10^{-13}\exp(-2470/T)$	3.55×10^{-17}
	NO_3 production from HNO_3 loss	
$HNO_3+OH \rightarrow NO_3+H_2O$	$R_1=2.4\times10^{-14}\exp(460/T)$	1.54×10^{-13}
	$R_2=2.7\times10^{-17}\exp(2199/T)$	
	$R_3=6.5\times10^{-34}\exp(1335/T)$ AIR	
	$R=R_1+R_3/(1+R_3/R_2)$	
	NO_3 production from N_2O_5 loss	
$N_2O_5+M \rightarrow NO_2+NO_3$	$R_1=10^{-3}$ (T/300)−3.5exp(−11000/T) AIR	5.02×10^{-2}
	$R_2=9.7\times10^{14}$ $(T/300)^{0.1}\exp(-11080/T)$	
	$F_c=0.35$	
N_2O_5 ($h\nu$) $\rightarrow NO_2+NO_3$		
	NO_3 loss	
$NO_3+NO_2 \rightarrow N_2O_5$ [b]	$R_1=3.6\times10^{-30}(T/300)^{-4.1}$ AIR	1.41×10^{-12}
	$R_2=1.9\times10^{-12}(T/300)^{0.2}$	
	$F_c=0.35$	
$NO_3+NO \rightarrow 2NO_2$	$1.8\times10^{-11}\exp(110/T)$	2.6×10^{-11}
$NO_3+NO_3 \rightarrow NO_2+NO_2+O_2$	$8.5\times10^{-13}\exp(-2450/T)$	2.3×10^{-16}
NO_3 ($h\nu$) $\rightarrow NO_2+O$		
NO_3 ($h\nu$) $\rightarrow NO+O_2$		
$NO_3+O \rightarrow NO_2+O_2$	1.7×10^{-11}	1.7×10^{-11}
$NO_3 \rightarrow NO+O_2$	1.4×10^{-4}	1.4×10^{-14}
	Reactions of NO_3 with RO_2 radicals	
$NO_3+HO_2 \rightarrow O_2+OH+O_2$	$4.\times10^{-12}$	4.0×10^{-12}
NO_3+RO_2 [a] $\rightarrow NO_2+HO_2$+product	2.3×10^{-12}	2.3×10^{-12}
	Reactions of NO_3 with unsaturated VOC	
$NO_3+C_2H_4 \rightarrow NO_3$ addition product	$3.3\times10^{-12}\exp(-2880/T)$	2.12×10^{-16}
$NO_3+C_3H_6 \rightarrow NO_3$ addition product	$4.6\times10^{-13}\exp(-1155/T)$	9.58×10^{-15}
NO_3+isoprene→addition product	$3.03\times10^{-12}\exp(-446/T)$	6.79×10^{-13}
NO_3+MVK→addition product	4.7×10^{-16}	4.7×10^{-16}
	HNO_3 production from NO_3 loss	
	Reactions of NO_3 with aldehydes	
$NO_3+HCHO \rightarrow HNO_3+CO+HO_2$	5.8×10^{-16}	5.8×10^{-16}
$NO_3+CH_3CHO \rightarrow HNO_3+RO_2$	$1.4\times10^{-12}\exp(-1900/T)$	2.4×10^{-15}
NO_3+MACR→HNO_3+product	3.7×10^{-15}	3.7×10^{-15}
	Reactions of NO_3 with DMS	
NO_3+DMS→HNO_3+radical	$1.9\times10^{-13}\exp(500/T)$	1.02×10^{-12}
	DMS reaction with OH radical (given here for comparison purposes)	
OH+DMS→addition products	$1.7\times10^{-42}\exp(7810/T)$ $[O_2])/(1+5.5\ 10^{-31}\exp(7460/T)$ $[O_2])$	1.8×10^{-12}
OH+DMS→abstraction products	$1.13\times10^{-11}\exp(-253/T)$	4.8×10^{-12}
	N_2O_5 loss to HNO_3	
$N_2O_5+H_2O \rightarrow 2HNO_3$	2.5×10^{-22}	2.5×10^{-22}
$N_2O_5+H_2O+H_2O \rightarrow 2HNO_3+H_2O$	1.8×10^{-39}	1.8×10^{-39}
	Other HNO_3 production	
$NO_2+OH \rightarrow HNO_3$ [b]	$R_1=2.6\times10^{-30}(T/300)^{-2.9}$ AIR	
	$R_2=4.1\times10^{-11}$	1.05×10^{-11}
	$F_c=0.4$	
	Other HNO_3 losses	
HNO_3 ($h\nu$) $\rightarrow NO_2+OH$		

[a]: R=CH_3, C_2 to C_5; 18 different RO_2 radicals [b]: $K=R_1/(1+R_1/R_2)$ F_c^A where $A=(1/(1+\log(R1/R2)^2)$

given in Table 4). On the basis of the k_4 and k_{-4} rates we can calculate the NO_2 levels at which the N_2O_5 concentrations equal those of NO_3. The calculated values (Table 3) are significantly higher than the geometric mean value of 0.4 ppbv of NO_2 observed during MINOS. Interestingly as shown in Table 3, during the entire period of the MINOS experiment, the typical time for the NO_3 conversion to N_2O_5 is 3 to 9 times slower than the thermal decomposition of N_2O_5 to NO_3. Thus, at high temperatures as those observed at Finokalia during the MINOS campaign, NO_3 is longer lived than N_2O_5 and consequently N_2O_5 is less effective as reservoir species for NO_3 contrary to what is expected at higher NO_2 levels and/or lower temperatures. Indeed, for the measured ranges of NO_2 and temperature, the equilibrium ratio N_2O_5/NO_3 ranges between 0.02 and below unity with an average value of 0.34($\pm$0.26). Only on the 13 August, this pattern is inversed with a N_2O_5/NO_3 ratio of 1.52 i.e. exceeding unity. During this particular day the site was influenced both by biomass burning as shown on the black carbon levels (Salisbury et al., 2003) and by subsidence of air masses with low RH. In Fig. 6a we depicted the correlation between NO_3 concentrations integrated over 1°C increments of temperature. Similar dependency is obtained between the lifetime of NO_3 and the temperature (Fig. 6b) indicating N_2O_5 loss dominance as observed and discussed by Geyer and Platt (2002).

In addition to temperature, RH varied by almost a factor of 4.5. Figure 6c presents both the variation of NO_3 radical and that of RH. It is interesting to note that the maximum NO_3 mixing ratio of 37 pptv has been observed on 11–12 August 2001 due to thermal dissociation of N_2O_5 and low heterogeneous removal when the RH was the lowest and the temperature was the highest observed during the experiment. To illustrate the influence of the relative humidity on NO_3 levels, the correlation between NO_3 and RH is presented in Fig. 6d, with NO_3 values integrated every 10 units of RH. A highly significant linear relationship is then observed with NO_3 decreasing by almost a factor of 3 when RH increases from 20–30% to 80–90% indicating the importance of both gas phase reactions of N_2O_5 with H_2O and reactions of N_2O_5 on particles since the hygroscopic growth of aerosols increases the surface available for heterogeneous reactions. This is also supported by the very good negative correlation between the lifetime of NO_3 and relative humidity shown in Fig. 6e. The lifetime of N_2O_5 with respect to the gas phase reactions with water into HNO_3 is reduced by a factor of 2 (from 46 to 23 min) when relative humidity increases from 35 to 85%, which could partly explain the observed negative correlation of NO_3 with relative humidity. However, a much faster removal of N_2O_5, probably by heterogeneous reactions, is needed to explain the calculated NO_3 lifetime of 1–6 min shown in Fig. 5c.

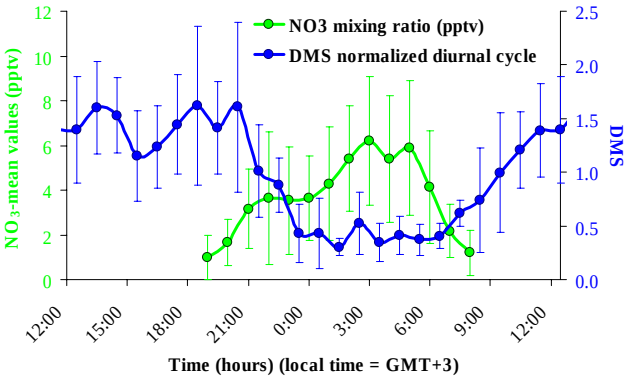

Fig. 7. Diurnal profile of NO_3 radical (in pptv) and normalized DMS concentrations (DMS concentrations divided by the corresponding diurnal mean DMS) averaged during the campaign.

3.4 Impact of DMS and others VOC on NO_3 oxidation

DMS is the dominant sulfur gas naturally emitted into the atmosphere. It is formed by biological processes in the sea water from dimethylsulfonioprionate (DMSP). The potential role of DMS in the CCN production but also in the acidity of rainwater in remote marine areas has been intensively studied since the publication of the CLAW hypothesis involving the influence of DMS oxidation products on climate (Charlson et al., 1987).

Platt and Le Bras (1997) suggested a potentially important role of DMS in the NO_x-NO_y partitioning in the marine background atmosphere. Cantrell et al. (1997) pointed out the contribution of NO_3 initiated oxidation of DMS to nighttime RO_2 formation. Allan et al. (1999, 2000) found that DMS levels can significantly affect the NO_3 lifetime. Especially under condition of elevated DMS (>100 pptv), a major fraction of NO_3 (up to 90%) is removed by reaction with DMS. During MINOS 2001, measurements of DMS were conducted in parallel with the NO_3 radical observations. As explained in Sect. 2.1, the NO_3 levels measured by the DOAS instrument correspond to a mean value within the first 150 m a.s.l whereas the DMS measurements have been performed at the sampling site 150 m a.s.l. However, during most of the campaign, the wind speed was higher than 5 m s^{-1} resulting in a well mixed MBL with height reaching 1000–1500 m (based on the radiosoundings performed every night at 3:00 LT at the Heraklion airport). Thus with only two exceptions (on the 13 and the 21 August) DMS is expected to be well mixed as has been observed at other marine sites (Davis et al., 1999). It is therefore reasonable to co-investigate the observed NO_3 and DMS variations. Figure 7 depicts the mean diurnal variation of NO_3 and of normalised DMS during MINOS campaign. The normalised DMS values were derived from the DMS concentrations divided by the corresponding diurnal mean DMS. The use of the normalised DMS values allows representing the diurnal

Table 5. Heterogeneous reactions taken into account in the model and the corresponding reactive accommodation coefficient (γ; T: temperature in K). $Khet=\gamma$ (RT/2πM)$^{0.5}$ A, where M is the molecular mass of the compound, A the aerosol surface area and R the gas constant. γ values are taken from Atkinson et al. (2003) (IUPAC recommendations web version 2003).
*close to the upper limit for the reaction.

	Reaction	γ
$Khet NO_3$	$NO_{3(g)} \rightarrow NO_{3(part)}$	0.006
$Khet 2NO_3$	$NO_{3(g)} \rightarrow HNO_{3(g)}$	$2.\times10^{-4}$
$Khet N_2O_5$	$N_2O_{5(g)} \rightarrow NO_{3(part)}$	0.1*
$Khet HNO_3$	$HNO_{3(g)} \rightarrow NO_{3(part)}$	0.0014
$Khet HO_2$	$HO_{2(g)} \rightarrow$ loss	5.66×10^{-5}exp(1560/T)

variation of the compound eliminating its day-to-day variability. Within about 3 h during and after sunset DMS decreases by a factor of about 6 when NO_3 radicals build up. This DMS decrease is due to both DMS oxidation by NO_3 leading to HNO_3 and dilution by continental air resulting to about 30% lower DMS fluxes during night (Bardouki et al., 2003a). Such a diurnal variation was observed during the entire campaign, and more details are reported in a companion paper (Bardouki et al., 2003). On the basis of the observed average NO_3, OH and DMS levels, DMS nighttime oxidation by NO_3 is about 75% the daytime loss by reaction with OH radicals. This is determined in further detail in Kanakidou et al. (2004, paper in preparation).

By considering the observed mean DMS concentration of 30 pptv during the campaign a lifetime of about 10^3 s is estimated for NO_3 radicals, which is significantly longer by almost a factor of 5–10 than that calculated during the campaign and depicted in Fig. 5c. NO_3 radicals can also be removed by a variety of VOCs especially by isoprene and terpenes. During the campaign isoprene levels were very low (about 7 pptv; Gros et al., 2003). No terpenes were measured during the campaign but their levels are expected to be very low since the surrounding vegetation is sparse and consists mainly of some dry herbs and low bushes. These results indicate that in Finokalia gas-phase reactions of DMS and most probably other VOCs with NO_3 radicals play a relatively minor role in the NO_3 budget and that most NO_3 is removed from the atmosphere via reactions of N_2O_5 with water vapour and/or NO_3 and N_2O_5 on aerosol surfaces.

3.5 Impact of NO_3 on HNO_3 formation

To investigate the NO_3 budget and to evaluate the NO_3 involvement in HNO_3 formation, box model simulations have been performed.

3.5.1 The model

The chemical scheme used for this purpose is based on Poisson et al. (2001) as updated by Tsigaridis and Kanakidou (2002) for the inorganic and hydrocarbon chemistry (up to C_5) including NO_3 radical reactions with peroxy radicals. Reaction rates have been updated according to Atkinson et al. (2003) (IUPAC-web version 2003) recommendations. Table 4 presents the gas phase reactions of NO_3 considered in the model. The N_2O_5 gas phase reactions with H_2O (1 and 2 order with respect to H_2O, Reaction 5a and b) are also considered as well as the heterogeneous reactions of NO_3, N_2O_5 and HNO_3 listed in Table 5. The sensitivity of the NO_3 calculated levels to the rates of the Reactions (5a) and (5b) has been studied on the basis of the IUPAC (Atkinson et al., 2003) and of the upper and lower limit JPL (Sander et al. 2003) recommendations. It has been found that the reported uncertainty in these rates can lead to up to a 0.5 pptv of uncertainty in the NO_3 calculated levels. Larger uncertainty is expected to be linked with the temperature dependence of these rates (up to 1.2 pptv) that is unfortunately not sufficiently documented (Dimitroulopoulou and Marsh, 1997). Deposition of HNO_3, NO_3, N_2O_5 and NO_3^- (particulate) onto surfaces has been considered with deposition velocities of 1 cm s^{-1} for the gases and 3 times higher for the particles since most $NO^-_{3(part)}$ is on coarse sea-salt particles (Bardouki et al., 2003b).

Observed hourly mean values of O_3, photolysis rates of NO_2 (JNO_2) and O_3 (JO^1D) and CO are used as input to the model that was also forced every 5-min by the geometric hourly mean values of NO_2 measured by the DOAS instrument. Missing NO_2 data have been substituted by extrapolating the observations on the basis of the diurnal mean normalized profile of NO_2 measured during the campaign. Isoprene, ethene, propene, formaldehyde, acetaldehyde, ethane, propane and butane mixing ratios are kept equal to 7, 100, 50, 1000, 100, 1000, 260 and 120 pptv respectively, according to observations during the MINOS campaign (Gros et al., 2003) and in the West Mediterranean (Plass-Dümler et al., 1992). Aerosol surfaces observed during the campaign (Bardouki et al., 2003a) are used to calculate the heterogeneous removal rates for the reactions listed in Table 5. Diurnal mean DMS observations were used to account for the DMS emitted by the ocean and its impact on NO_3 chemistry in the marine boundary layer. DMS oxidation both by OH radical and by NO_3 radical is taken into account (see reaction rates in Table 4). Initial concentrations of hydrogen peroxide (495 pptv), methane (1.8 ppmv) and particulate nitrate (25 nmol m^{-3}) are applied.

3.5.2 Model results

Note that since hourly mean data are used as input to the model for most species, our simulations are not expected to provide reliable higher time resolution variability. The model

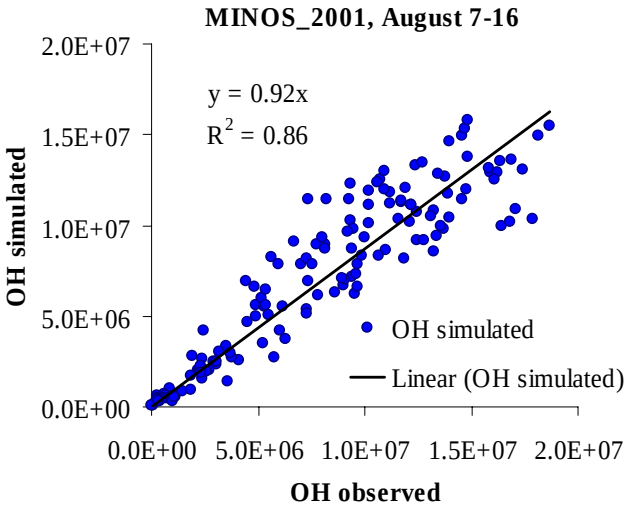

Fig. 8. Correlation between the modelled and measured OH concentrations during the campaign.

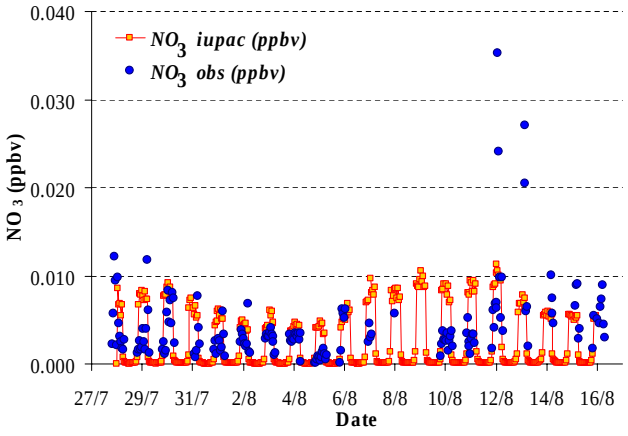

Fig. 9. Comparison between the modelled (orange line) and measured NO_3 (closed circles) hourly mean levels (in ppbv) during the campaign.

satisfactorily simulates the daytime variation and the absolute concentrations of OH radicals as shown in Fig. 8, although overall it underestimates the observations of OH radical by about 8%. Details of OH radical measurements are reported by Berresheim et al. (2003).

NO_3 model versus observations. NO_3 radical concentrations simulated by the model for the whole period are shown in Fig. 9 together with the observed NO_3 values (hourly mean). When neglecting the NO_3 values observed during the nights of 11 to 12 and 12 to 13 of August 2001 that are exceptionally high for the measuring period the model results seem to capture the order of magnitude of the observations within the range of their variability. Note that during these days biomass burning activities have affected the site as indicated by the CO observed levels and relevant compounds (Salisbury et al., 2003). In addition, the very low RH observed on the 8 and the 13 August and linked to low aerosol surfaces (Bardouki et al., 2003a) indicates subsidence of air masses from higher altitudes. This transport mechanism can not be reproduced by the box model. Although, the mean NO_3 concentration of 4.5 pptv (all data) observed during night is in quite good agreement with the 4.7 pptv simulated by the model for the same period, there is no statistically significant correlation between the hourly averaged observed concentrations and the hourly calculated NO_3

Losses of NO_3. According to our calculations photolysis of NO_3 is by far the major loss mechanism during daytime since it accounts for more than half the total removal of NO_3 and N_2O_5. The loss of NO_3 by the reaction with NO is half that due to photolysis. During night the relative importance of the various paths of NO_3 and N_2O_5 loss is changing but generally N_2O_5 heterogeneous and gas phase losses (to molecules other than NO_3) are almost a factor of 2 higher than the reaction of NO_3 with DMS. This relatively small contribution of DMS to NO_3 loss (less than 25%) compared to earlier published estimates by Carslaw et al. (1997) reflects the different conditions encountered during the studies with regard to the DMS levels (the lowest have been observed during MINOS) and the different durations of nighttime, when this reaction is important (shortest during our study). Under the studied conditions the reactions of other VOCs with NO_3 seem to be of minor importance in controlling the NO_3 budget.

HNO_3 and NO_3^- (particulate) model versus observations. The contribution of NO_3 nighttime reactions with VOC (including DMS), leading to HNO_3 formation has also been investigated on the basis of the model results. The model simulates within 10% the observed levels of the sum of the gaseous HNO_3 and the particulate NO_3^- ($NO_{3(part)}$). The best agreement is achieved for the period 28 July to 1 August 2001 (Fig. 10a). Thus, to investigate the NO_3 involvement in the HNO_3 production, we focus on this first period of the campaign when the model appears to realistically simulate HNO_3 levels.

According to our calculations HNO_3 is predominantly formed during daytime by reaction of NO_2 with OH at a rate of 1.12 ppbv/d. DMS oxidation by NO_3 radicals is an important source of HNO_3 during night, producing 0.11 ppbv/d of HNO_3 whereas 0.10 ppbv/d of HNO_3 is formed from the gas phase reactions of N_2O_5 with water vapour. The NO_3 heterogeneous reaction appears to be minor since it does not produce more than 1 pptv/d of HNO_3. The overall HNO_3 production is calculated to be 1.3 ppbv/d. NO_3 and N_2O_5 gas phase reactions constitute the nighttime chemical source for HNO_3 and contribute therefore approximately 16% to the HNO_3 production (Fig. 10b). Under the studied conditions, the reactions of NO_3 with aldehydes are minor for HNO_3 production since only 3 and 1 pptv/d are produced during the NO_3 initiated oxidation of formaldehyde

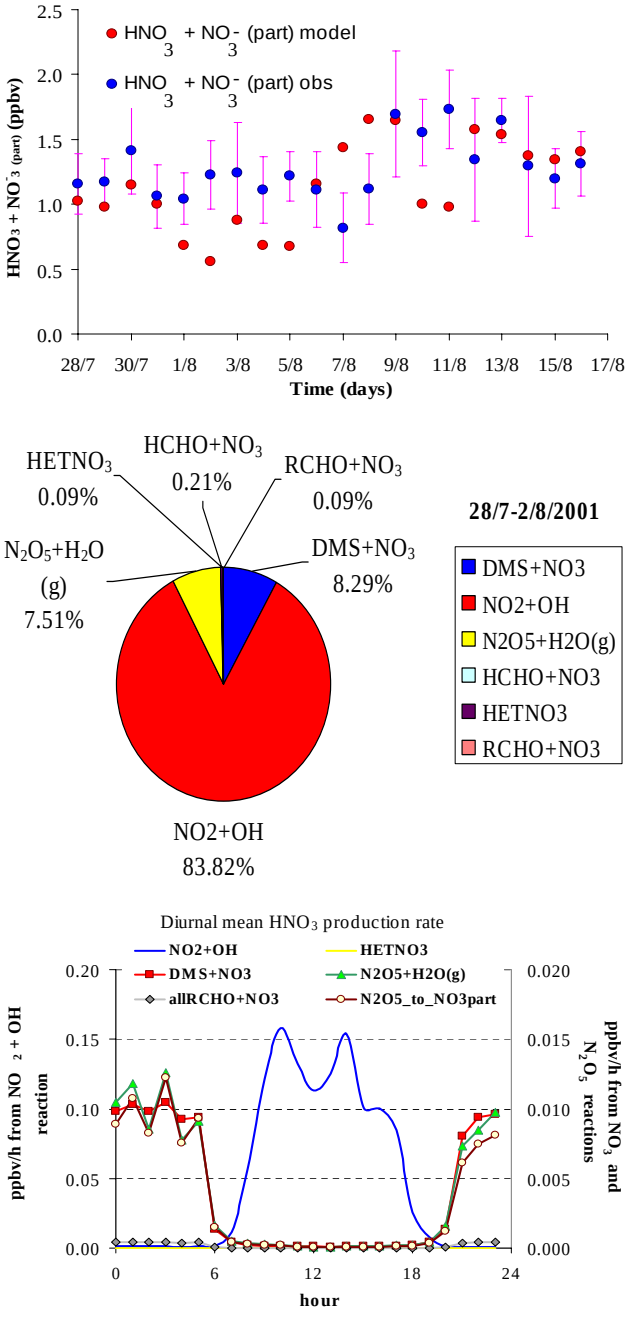

Fig. 10. (a) Comparison between the calculated and observed sum of $HNO_{3(g)}$ and $NO_{3(part)^-}$ concentartions. **(b)** Distribution of HNO_3 (gaseous) formation; **(c)** diurnal mean HNO_3 production rate. Note the difference of a factor of 10 in the scale for the NO_2+OH reaction rate (axis to the left) compared to the other reactions (axis to the right).

and higher aldehydes respectively. Figure 10c depicts the mean diurnal variation of the HNO_3 production rates, which reveals the importance of the NO_3 and N_2O_5 reaction for HNO_3 formation during nighttime.

The calculated HNO_3 daytime production rate of 1.12 ppbv/d during the MINOS campaign is more than double that suggested by Carslaw et al. (1997) for lower photochemical activity conditions (less OH radicals than during MINOS). However, the DMS contribution to HNO_3 formation via H-abstraction by NO_3 radicals is lower than the estimate by Carslaw et al. (1997). This difference is due to high DMS concentrations that resulted from a phytoplankton bloom in the area studied by these authors. Thus our results, although different from those in that earlier study, are fully consistent when taking into account the different conditions of the studied environments.

The heterogeneous reaction of N_2O_5 (γ=0.1) on particles does not produce more than 0.09 ppbv/d of particulate NO_3^- ($NO_{3(part)}^-$). Therefore, by considering the overall $HNO_{3(g)}$+$NO_{3(part)}^-$ production, N_2O_5 and NO_3 reactions contribute up to 21%, whereas the remaining is attributed to the NO_2 reaction with OH during daytime.

With regard to HNO_3 loss from the atmosphere, reaction with OH and photolysis are calculated to play only a minor role in the total loss of HNO_3 (2% and 1% respectively) whereas its main removal mechanism (97%) is conversion to particulate NO_3^- and subsequent deposition.

4 Conclusions

During the MINOS campaign from 27 July to 17 August 2001, a complete set of NO_3 data was obtained by a DOAS instrument with NO_3 levels that vary from the detection limit up to 37 pptv. The 24-hour mean NO_3 levels were a factor of 12 higher than these of the OH radical. Thus for some compounds such as DMS, the nighttime destruction by NO_3 is much more important than by OH during daylight. The role of NO_3 for the overall oxidation efficiency of the Mediterranean atmosphere on a yearly basis is a topic for further research since preliminary measurements show a much smaller seasonal variation for NO_3 compared to OH radicals.

The calculated lifetime of NO_3 during the MINOS campaign range between 1 and 6 min, supporting the assumption of steady state conditions between production and destruction of NO_3. Gas-phase reactions of DMS and other VOCs with NO_3 radicals appear to play a minor role in the NO_3 budget, since the major fraction of NO_3 is removed from the atmosphere via N_2O_5 reactions.

NO_3 radical as well as its lifetime was found to be strongly anti-correlated with the relative humidity (RH). High values of RH are associated with efficient loss of NO_3, reducing it to levels down to the detection limit. This indicates that both gas phase reactions of N_2O_5 with H_2O and reactions of NO_3 and N_2O_5 on particles are important since the hygroscopic growth of aerosols increases the surface available for heterogeneous reactions.

N_2O_5 and NO_3 reactions contribute up to 21% to the total formation rate of $HNO_{3(g)}$+$NO_{3(part)}^-$, while the remaining

and thus major part is attributed to the NO_2 reaction with OH during daytime. The contribution of N_2O_5 and NO_3 reactions to the overall $HNO_{3(g)}$+$NO^-_{3(part)}$ production on a seasonal basis deserves further study.

Acknowledgements. We wish to thank T. Klupfel for assistance with the DOAS instrument, M. Martinez-Harder for useful comments on DOAS measurements, H. Bardouki, V. Gros, G. Kouvarakis, K. Oikonomou and J. Sciare for communicating the DMS, HNO_3, $NO^-_{3(part)}$ and VOC data prior publication, Prof. U. Platt for helpful discussions, the Greek secretary of research and Technology for financial support of M. Vrekoussis (PENED grant) and the two anonymous reviewers for their fruitful remarks. M. Vrekoussis acknowledges support by DAAD for educational visits to MPI-Mainz.

References

Allan, B. J., Carslaw, N., Coe, H., Burgess, R., and Plane, J. M. C.: Observations of the Nitrate Radical in the marine boundary layer, J. Atmos. Chem., 33, 129–154, 1999.

Allan, B. J., Mc Figgans, G., Plane, J. M. C., Coe, H. and Mc Fadyen, G. G.: The nitrate radical in the remote marine boundary layer, J. Geophys.Res., 105, D19, 24 191–24 204, 2000.

Atkinson, R.: Kinetic and mechanism of gas-phase reactions of NO_3 radical with organic compounds, J. Physical Chem., 20, 459–507, 1991.

Atkinson, R., Baulch, D. L., Cox, R. A., Crowley, J. N., Hampson, R. F., Kerr, J. A., Rossi, M. J., and Troe, J.: IUPAC recommendations, Web version: http://www.iupac-kinetic.ch.cam.ac.uk/, 2003.

Bardouki, H., Berresheim, H., Vrekoussis, M., Sciare, J., Kouvarakis, G., Oikonomou, C., Schneider, J., and Mihalopoulos, N.: Gaseous (DMS, DMSO, SO_2, H_2SO_4, MSA) and particulate (MS^- and SO^{2-}_4) sulfur compounds during the MINOS campaign, Atmos. Chem. Phys., 3, 1871–1886, 2003a.

Bardouki, H., Liakakou, H., Economou, C., Sciare, J., Smolik, J., Zdimal, V., Eleftheriadis, K., Lazaridis, M., Dye, C., and Mihalopoulos, N.: Chemical composition of size-resolved atmospheric aerosols in the eastern Mediterranean during summer and winter, Atmos. Environ., 37, 195–208, 2003b.

Berresheim, H., Elste, T., Plass-Dülmer, C., Eisele, F. L., and Tanner, D. J.: Chemical ionization mass spectrometer for long-term measurements of atmospheric OH and H_2SO_4, Int. J. Mass Spectrom., 202, 91–103, 2000.

Berresheim, H., Plass-Dülmer, C., Elste, T., Mihalopoulos, N., and Rohrer, F.: OH in the coastal boundary layer of Crete during MINOS: Measurements and relationship with ozone photolysis, Atmos. Chem. Phys., 3, 639–649, 2003.

Brauers, T., Hausmann, M., Brandenburger, U., and Dorn, H.-P.: Improvement of Differential Optical Spectroscopy with a multichannel scanning technique, Appl. Opt., 34, 4472–4479, 1995.

Cantrell, C. A., Shetter, R. E., Calvert, J. G., Eisele, Fl., and Tanner, D. J.: Some considerations of the origin of nighttime peroxy radicals observed in MILOPEX 2c, J. Geophys. Res., 102, 15 899–15 913, 1996.

Carslaw, N., Plane, J. M. C., Coe, H., and Cuevas, E.: Observation of the nitrate radical in the free troposphere., J. Geophys.Res., 102, D9, 10 613–10 622, 1997.

Charlson, R. J., Lovelock, J. E., Andreae, M. O., and Warren, S. G.: Oceanic phytoplankton, atmospheric sulphur, cloud albedo and climate: a geophysiological feedback, Nature, 326, 655–661,1987.

Cofer III, W. R., Collins, V. G., and Talbot, R. W.: An improved aqueous scrubber for the collection of soluble atmospheric trace gases, Environ. Science Technology, 19, 557–560, 1985.

Davis, D., Chen, G., Bandy, A., Thornton, D., Eisele, F., Mauldin, L., Tanner, D., Lenschow, D., Fuelberg, H., Huebert, B., Heath, J., Clarke, A., and Blake, D.: Dimethyl sulfide oxidation in the equatorial Pacific: Comparison of model simulations with field observations for DMS, SO_2, $H_2SO_{4(g)}$, $MSA_{(g)}$, and MS, and NSS, J. Geophys. Res., 104, 5765–5784, 1999.

DeMore, W. B., Sander, S. P., Golden, D. M., Hampson, R. F., Kyrylo, M. J., Howard, C. J., Ravishankara, A. R., Kolb, C. E., and Molina, M. J.: Chemical kinetics and photochemical data for use in stratospheric modeling, Eval. 11, Jet Propul. Lab., Pasadena, Calif., 1997.

Dimitroulopoulou, C. and Marsh, A. R. W.: Modelling studies of NO_3 nighttime chemistry and its effects on subsequent ozone formation, Atmos. Environ., 31, 3041–3057, 1997.

Geyer, A., Ackermann, R., Dubois, R., Lohrmann, B., Muller, T., and Platt, U.: Long term observation of Nitrate radicals in the continental layer near Berlin., Atmos. Environ., 35, 3619–3631, 2001.

Geyer, A. and Platt, U.: Temperature dependence of the NO_3 loss frequency: A new indicator for the contribution of NO_3 to the oxidation of monoterpenes and NO_x removal in the atmosphere, J. Geophys. Res., 107, D20, 4431, doi:10.1029/2001JD001215, 2002.

Gros, V., Williams, J., van Aardenne, J. A, Salisbury, G., Hofmann, R., Lawrence, M. G., von Kuhlmann, R., Lelieveld, J., Krol, M., Berresheim, H., Lobert, J. M., and Atlas, E.: Origin of anthropogenic hydrocarbons and halocarbons measured in the summertime european outflow (on Crete in 2001) Atmos. Chem. Phys., 3, 1223–1235, 2003.

Heintz, F., Platt, U., Flentje, H., and Dubois, R.: Long term observation of Nitrate radicals at the Tor Stations, Kap Arkona (Rügen), J. Geophys. Res., 101, D17, 22 891–22 910, 1996.

Kouvarakis, G. and Mihalopoulos, N.: Seasonal variation of dimethylsulfide in the gas phase and of methanesulfonate and non-sea-salt sulfate in the aerosol phase measured in the eastern Mediterranean atmosphere, Atmos. Environ., 36, 929–938, 2002.

Martinez, M., Perner, D., Hackenthal, E., Kultzer, S., and Schultz, L.: NO_3 at Helgoland during the NORDEX campaign in October 1996, J. Geophys. Res., 105, D18, 22 685–22 695, 2000.

Martinez-Harder, M.: Messungen von BrO und anderen Spurenstoffen in der bodennahen Troposphare, Ph.D Thesis, Max Planck-Institute for Chemistry, Mainz, 1998.

Mentel, Th. F., Bleilebens, D., and Wahner, A.: A study of nighttime nitrogen oxide oxidation in large reaction chamber – The fate of NO_2, N_2O_5, HNO_3 and O_3 at different humidities, Atmos. Environ, 30, 23, 4007–4020, 1996.

Platt, U. and Le Bras, G.: Influence of DMS on the NO_x-NO_y partitioning and the NO_x distribution in the marine backgraound atmosphere, Geophys. Res. Letters, 24, 1935–1938, 1997.

Platt, U., Winer, A. M., Biermann, H. W., Atkinson, R., and Pitts, J.: Measurements of nitrate radical concentrations in continental air, Environ. Science Technology, 18, 365–369, 1984.

Platt, U., Perner, D., Harris, G. W., Winer, A. M., and Pitts, J. M.: Detection of NO_3 in the polluted troposphere by differential optical absorption, Geophys. Res. Letters, 7, 89–92, 1980.

Plass-Dümler, C., Ratte, M., Koppmann, R., and Rudolph, J.: C2-C9 Hydrocarbons in the Marine atmosphere during NATAC 91, paper presented at the NATAC 91 workshop, Odessa, Ukraine, 1992.

Poisson, N., Kanakidou, M., Bonsang, B., Behmann, T., Burrows, J. P., Fischer, H., Golz, C., Harder, H., Lewis, A., Moortgat, G. K., Nunes, T., Pio, C. A., Platt, U., Sauer, F., Schuster, G., Seakins, P., Senzig, J., Seuwen, R., Trapp, D., Volz-Thomas, A., Zenker, T., and Zitzelberger, R.: The impact of natural non-methane hydrocarbon oxidation on the free radical and ozone budgets above a eucalyptus forest, Chemosphere: Global Change Science, Elsevier Science, 3, 353–366, 2001.

Salisbury, G., Williams, J., Holzinger, R., Gros, V., Mihalopoulos, N., Vrekoussis, M., Sarda-Estève, R., Berresheim, H., von Kuhlmann, R., Lawrence, M., and Lelieveld, J.: Ground-based PTR-MS measurements of reactive organic compounds during the MINOS campaign in Crete, July–August 2001, Atmos. Chem. Phys. 3, 925–940, 2003.

Sander, S. P., Friedl, R. R., Ravishankara, A. R., Golden, D. M., Kolb, C. E., Kurylo, M. J., Huie, R. E., Orkin, V. L., Molina, M. J., Moortgat, G. K., and Finlayson-Pitts, B. J.: Chemical Kinetics and Photochemical Data for Use in Atmospheric Studies, Evaluation Number 14, JPL, Publication 02-25, February 2003.

Sciare, J. and Mihalopoulos, N.: Atmospheric Dimethylsulfoxide (DMSO): An improved method for Sampling and analysis. Atmos. Environ., 34, 151–156, 2000.

Sverdrup, G. M., Spicer, C. W., and Ward, G. F.: Investigation of the gas-phase reaction of dinitrogen pentoxide with water-vapor, Int. J. Chem. Kinet., 19, 191–205, 1987.

Tsigaridis, K. and Kanakidou, M.: Importance of Volatile Organic Compounds Photochemistry Over a Forested Area in Central Greece, Atmos.Environ., 36, 19, 3137–3146, 2002.

Wahner, A., Mentel, T. F., and Sohn, M.: Gas-phase reaction of N_2O_5 with water vapour: importance of heterogeneous hydrolysis of N_2O_5 and surface deposition of HNO_3 in a large Teflon chamber, Geophys. Res. Letters, 25, 2169–2172, 1998a.

Waengberg, I., Etzkorn, T., Barnes, I., Platt U., and Becker, K.: Absolute determination of the temperature behavior of the NO_2+NO_3^-+(M)→N_2O_5+(M) equilibrium, J. Phys. Chem. A, 101, 9694–9698, 1997.

Wayne, R. P., Barnes, I., Biggs, P., Burrows, J. P., Canasa-Mas, C. E., Hjorth, J., Le Bras, G., Moorgat, G. K., Perner, D., Poulet, G., Restelli, G., and Sidebottom, H.: The nitrate radical physics, chemistry, and the atmosphere., Atmos. Environ., 25A, 1–203, 1991.

Yokelson, R. J., Burkholder, J. B., Fox, R. W., Talukdar, R. K., and Ravisankara, A. R.: Temperature dependence of the NO_3 radical, J. Phys. Chem. 98, 13 144–13 150, 1994.

Yoshino, K., Esmond., J. R., and Parkinson, W. H.: High resolution absorption cross section measurements of NO_2 in the UV and VIS region, Chemical Physics, 221, 169–174, 1997.

Yvon, S. A., Plane, J. M. C., Nien, C.-F., Cooper, D. J., and Saltzman, E. S.: Interaction between nitrogen and sulphur cycles in the polluted marine boundary layer, J. Geophys. Res., 101, 3, 1379–1386, 1996.